

PACS numbers: 42.55.Rz; 42.65.Re
DOI: 10.1070/QE2002v032n06ABEH002233

Femtosecond Cr^{4+} : forsterite laser pumped by ytterbium-doped fibre laser and its noise characteristics

V.M. Gordienko, A.A. Ivanov, A.N. Konovalov, A.A. Podshivalov, V.I. Pryalkin, A.B. Savel'ev

***Abstract*. A femtosecond Cr^{4+} : forsterite laser is fabricated which is pumped by a PYL-10-LP fibre laser and generates a continuous train of 45-fs pulses with a repetition rate of 110 MHz and an average output power of 250 mW. The noise spectra of the femtosecond and solid-state pump lasers are studied.**

Keywords: *femtosecond laser, solid-state lasers, noise characteristics.*

1. Introduction

Femtosecond laser technologies are being recently rapidly incorporated in the studies in physics, chemistry, and biology and also have a number of technological applications. Typical examples are optical coherent tomography [1, 2], femtosecond metrology [3], nonlinear laser microscopy [4], etc. The problems of femtosecond laser technology are regularly considered on conferences [5] and have been recently discussed in Quantum Electronics [6].

The dynamics of development of femtosecond technologies is determined by the technical possibilities of modern femtosecond lasers and by their commercial availability. Ti : sapphire lasers are most popular at present. Commercially available femtosecond lasers manufactured by Coherent and Spectra-Physics produce femtosecond pulses of duration less than 50 fs with an average output power of 1 W.

A Cr^{4+} : forsterite ($Cr^{4+} : Mg_2SiO_4$) crystal is a promising active medium for femtosecond lasers [7 – 11]. The width of the fluorescence band of Cr^{4+} : forsterite is 195 nm, which allows in principle producing pulses of duration down to 10 fs [8]. The possibilities of wide applications of femtosecond Cr^{4+} : forsterite lasers were discussed in Ref. [11]. These lasers are pumped, as a rule, by radiation in the wavelength range between 1000 and 1100 nm emitted by Nd-doped solid-state lasers, in particular, $Nd : YVO_4$.

V.M. Gordienko, A.N. Konovalov, A.A. Podshivalov, V.I. Pryalkin, A.B. Savel'ev Department of Physics, M.V. Lomonosov Moscow State University, Vorob'evy gory, 119899 Moscow, Russia;
A.A. Ivanov Center of Photochemistry, Russian Academy of Sciences, ul. Novatorov 7a, 117421 Moscow, Russia

Received 28 March 2002
Kvantovaya Elektronika **32** (6) 511 – 515 (2002)
Translated by M.N. Sapozhnikov

The use of an ytterbium-doped fibre laser for pumping a Cr^{4+} : forsterite crystal [9] opens up new prospects because a noticeable progress has been recently achieved in the manufacturing of these lasers. Fibre lasers are compact, they feature a sufficiently high conversion efficiency (above 60 %), and their output power exceeds 10 W for an operating life more than 10^4 hours [13]. In addition, a high quality of the laser beam emitted from a fibre and a high stability of the laser provide a convenient and reliable coupling of its radiation to the resonator of a femtosecond laser.

In this paper, we discuss the power, spectral, temporal, and noise characteristics of a femtosecond Cr^{4+} : forsterite laser with parameters controlled in real time, which we manufactured using domestic elemental base [12].

2. Femtosecond Cr^{4+} : forsterite laser

We used in our study a PYL-10-LP fibre laser (IRE-Polyus Research and Production Association) as a pump source [13]. The output power of this laser amounts to 10.6 W for the TEM_{00} transverse mode and a linear polarisation of radiation with the discrimination degree of more than 50 : 1. The fibre output (the fibre length was 3 m) permits the delivering of collimated radiation (the beam diameter was 2.9 mm) directly to a lens focusing the pump radiation into an active element, which substantially increases the stability of femtosecond lasing.

Fig. 1 shows the optical scheme of the Cr^{4+} : forsterite laser. The resonator has a classical Z scheme. The active element is a Cr^{4+} : forsterite crystal of length 19 mm with the absorption coefficient of about 1 cm^{-1} at the pump radiation wavelength of 1063 nm. The crystal is mounted in a monoblock cooled with a Peltier element whose temperature is controlled with a microcontroller. The laser resonator is formed by mirrors (*3 – 6*). Mirror (*7*) is used for laser adjusting and obtaining cw lasing. Beamsplitter (*10*) deflects a part of output radiation for measuring its parameters.

To control the laser parameters, we developed an automated system that included an autocorrelator for measuring duration of femtosecond pulses in the range from 30 to 200 fs, a spectrometer for measuring the laser emission spectrum in the spectral range from 1200 to 1300 nm, a power meter for measuring an average power of femtosecond radiation in the range from 1 mW to 1 W and pump radiation power in the range from 1 to 10 W, as well as a device for thermal control of the Cr^{4+} : forsterite crystal.

The system for control of laser-radiation parameters is mounted on a separate platform and is located on the

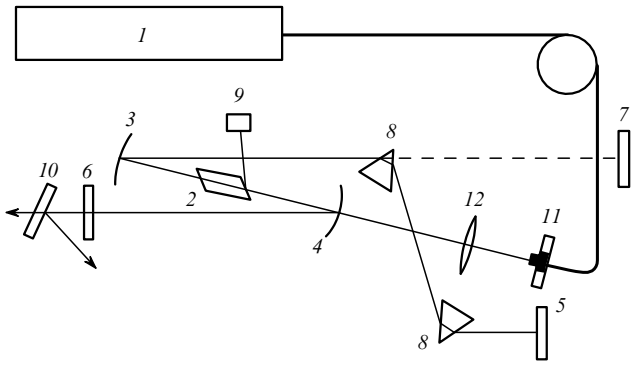

Figure 1. Scheme of the Cr^{4+}:forsterite laser: (*1*) PYL-10-LP fibre pump laser with a fibre radiation outcoupler; (*2*) active element; (*3–6*) resonator mirrors (the reflectivity of mirrors (*3–5*) and (*6*) in the 1200–1300-nm range is 100 % and 92 %, respectively; mirror (*4*) is dichroic (with transmission more than 85 % at 1063 nm); (*7*) auxiliary mirror; (*8*) prisms; (*9*) photodetector for measuring the average pump energy; (*10*) beamsplitter; (*11*) holder of a fibre outcoupler of the pump laser; (*12*) focusing lens.

supporting plate of the laser. The optical scheme of the system is shown in Fig. 2. A phase plate rotates the polarisation plane of the incident beam so that it makes an angle of 45° with the principal planes of delay-line crystals. Mirror (*2*) reflects 90 % of radiation to the measuring tract of the correlator, where the radiation passes through crystal (*6*) in the constant delay line and crystal (*7*) in the delay line (mounted on a rotation stage controlled with a step motor). Having been reflected from mirror (*4*), radiation passes again through both crystals in the delay line, is reflected by mirror (*5*), and focused by lens (*8*) into a DKDP crystal (*9*) of thickness 200 μm, which is cut in the direction of type II SHG phase matching for radiation at 1250 nm. The second harmonic radiation energy is measured with photodetector (*11*) through filter (*10*) rejecting the fundamental radiation. The radiation transmitted through mirror (*2*) is reflected from mirror (*3*) to a 600 lines mm^{-1} diffraction grating, which is also mounted on the rotation stage. The radiation transmitted through mirror (*3*) is measured with photodetector (*11*), whose output signal is proportional to the average power of femtosecond radiation.

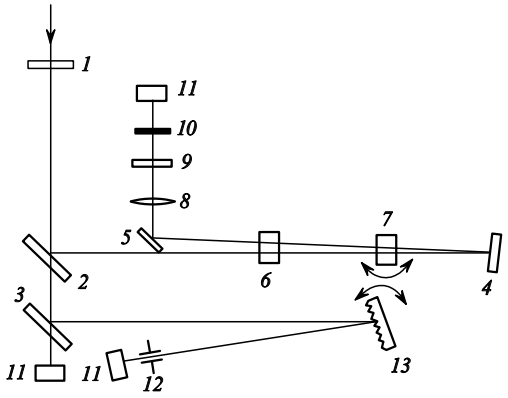

Figure 2. Optical scheme of the correlator-spectrometer: (*1*) phase plate; (*2–5*) deflecting mirrors; (*6*) PDL crystal; (*7*) VPDL crystal; (*8*) focusing lens; (*9*) SHG DKDP crystal; (*10*) filter; (*11*) photodetectors; (*12*) diaphragm; (*13*) diffraction grating.

A step motor provides a simultaneous rotation of the delay-line crystal and the diffraction grating. The radiation diffracted from the grating is incident on InGaAs photodetector (*11*) in front of which slit (*12*) of width 100 μm is mounted. The resolution of this spectrometer is 1 nm for a distance between the grating and slit of 30 cm. The spectrometer was calibrated using the 1063-nm pump line and the 1250-nm line of the Cr^{4+}:forsterite laser.

The operation of the autocorrelator for determining the pulse duration is based on the measurement of the second harmonic energy upon the eo–e interaction when two replicas of the fundamental radiation pulse of the o- and e-polarisations are mutually delayed [14]. A second-order cross-correlation function obtained in this case unambiguously determines the fundamental-pulse duration if the thickness of a SHG crystal is much smaller than the group length of the type II phase-matching interaction between the fundamental and second harmonic pulses. A DKDP crystal features the minimum group-velocity dispersion in the spectral range from 1230 to 1270 nm (a two-fold dispersion spread of a 50-fs pulse occurs over the crystal length of above 5 cm). The minimum group length for the type II SHG (the oe–e interaction) is 0.53 mm for a 50-fs pulse. This means that such a correlator can measure the pulse duration down to 20 fs in crystals of length 200 μm.

We measured the average power of the second harmonic generated in a SHG crystal in the presence of two fundamental pulses with o- and e-polarisations, which were preliminary separated and mutually delayed in a birefringent crystal in the polarisation delay line (PDL) (a DKPD crystal of thickness 5 mm, which was cut in the direction $\theta = 45°$). Femtosecond pulses were made coincident in time in the SHG crystal with the help of a variable polarisation delay line (VPDL), in which a similar DKDP crystal was used, which was oriented so that its optical axis was orthogonal to that of the PDL crystal. Upon rotation of the VPDL crystal in the principal optical plane within a narrow angular interval ($45 \pm 10°$), the e-polarisation pulse is delayed by -150 – $+150$ fs relative to the o-polarisation pulse after passing through the crystal.

Thus, by angular scanning the VPDL crystal with a step motor and measuring the second harmonic pulse energy, we can determine the cross-correlation function of a laser pulse. The shape of this function depends on the mutual orientation of polarisation of the incident radiation and the principal plane of the SHG crystal. If the angle between the polarisation plane of one of the incident beams and the principal plane is zero, a smooth cross-correlation function without any pedestal is obtained. For the 45° orientation, the correlation function exhibits the 100 % modulation and a pedestal. In the case of intermediate orientations, the pedestal level and the modulation degree vary. Fig. 3 shows an example of the correlation function for the 5° orientation. The oscillation period on the curve corresponds to a change in the relative delay by 4.2 fs for lasing at 1260 nm.

The output signals of photodetectors of the spectrometer, autocorrelator, and power meters were digitised and read out with a microprocessor, which also controlled the step motor. The number of accumulated pulses for each position of the latter was programmed. For a maximum operating frequency of the step motor equal to 5 kHz, the duration of a sampling consisting of 1000 points (upon scanning in the range of 1000 nm) without accumulation is 0.2 s. The information is displayed faster when the scanning

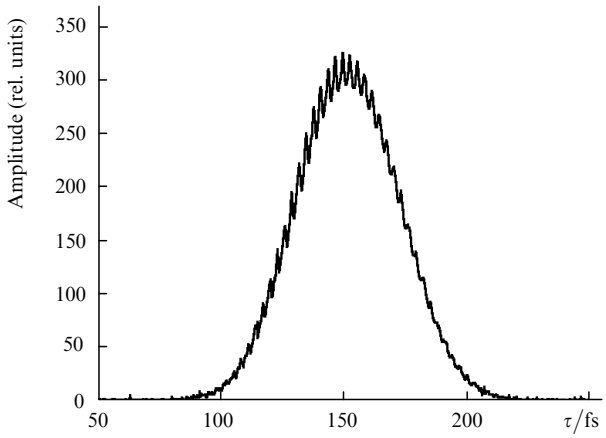

Figure 3. Correlation function of a pulse from the femtosecond Cr^{4+} : forsterite laser.

range is narrower. The microprocessor provides a preliminary signal processing and data transfer to a PC via a standard serial port. Software based on the Lab View packet provides the data processing and real-time control of periphery devices. Fig. 5 shows an image on the PC monitor produced by the detection system.

Because the gain in a Cr^{4+} : forsterite crystal depends on temperature, we developed a thermal stabilisation system. The crystal temperature was maintained with an accuracy of $\pm 0.1^{\circ}$ by means of a thermoelectric element, whose hot junction was cooled by water in a continuos-flow cooling unit. The minimum temperatures of the active element (for cooling water temperature of 13 °C) were −10 and −20 °C for pump powers of 9 and 5 W, respectively. The temperature dependence of the output power of femtosecond radiation is shown in Fig. 4. One can see that the output power of the Cr^{4+} : forsterite laser increases linearly with decreasing crystal temperature. However, to cool the crystal below the dew point, it should be blown off by dry nitrogen. For this reason, we chosen the operation temperature range from 5 to 7 °C. Under such conditions and a pump power of ~8 W, no water vapours were precipitated on the crystal surface.

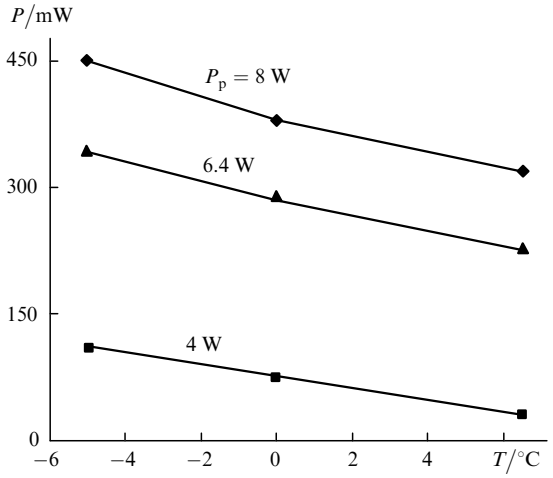

Figure 4. Temperature dependences of the average output power P of femtosecond radiation for different pump powers P_p.

The output characteristics of the Cr^{4+} : forsterite laser depended on its adjustment. The minimum pulse duration was 45 fs for an average output power of 250 mW and a pulse repetition rate of 110 MHz. For 70-fs pulses, the output power increased up to 380 mW. The general view of the Cr^{4+} : forsterite laser developed by us is shown in Fig. 5.

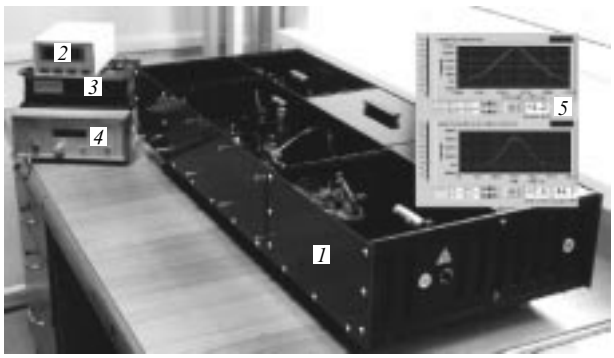

Figure 5. General view of the femtosecond Cr^{4+} : forsterite laser: (*1*) laser housing containing the resonator and detection system; (*2*) thermal stabilisation system; (*3*) PYL-10-LP fibre laser; (*4*) power supply of the PYL-10-LP laser; (*5*) image on the monitor of a detection system with parameters of femtosecond radiation.

3. Measurement of noise parameters

One of the important applications of femtosecond lasers is precision heterodyne measurements [1, 2]. However, the potential possibilities of such measurements are determined not only by the pulse duration and the output power but also by the output stability. We studied experimentally the amplitude noises of the femtosecond and pump lasers. For comparison, we also measured the noise parameters of the Cr^{4+} : forsterite laser pumped by a Millennia-IR laser.

The radiation from the lasers was incident on a photodetector, whose output signal was fed to an oscilloscope and a C4-74 spectrum analyser connected to a PC, which provided the averaged noise spectra. The noise spectra were recorded both upon cw and mode-locked lasing. The modulation degree was detected with an oscilloscope.

The averaged values of the modulation degree of the envelope of the femtosecond pulse train were coincident by the order of magnitude for pumping by the Millennia-IR and PYL-10-LP lasers, being 0.075 ± 0.025 % ($\sim 7.5\times10^{-4}$) and 0.2 ± 0.1 % ($\sim 2 \times 10^{-3}$), respectively. The spectral characteristics of amplitude noises were substantially different. Fig. 6 shows the corresponding averaged spectra of the amplitude noise for femtosecond lasers and corresponding pump lasers. One can see that noises of the femtosecond laser pumped by the Millennia-IR laser are localised in the low-frequency region (up to 20–30 kHz), whereas noises observed upon pumping by the PYL-10-LP fibre laser have a broader spectrum and are located in the high-frequency band from 30 to 150 kHz.

The spectral density of the noise of the femtosecond laser pumped by the Millennia-IR solid-state laser in the range from zero to 20 kHz is approximately ten times higher than that of the laser pumped by the fibre laser. However, at frequencies above 150 kHz, the situation is reversed: the noise density upon pumping by the Millennium-IR laser

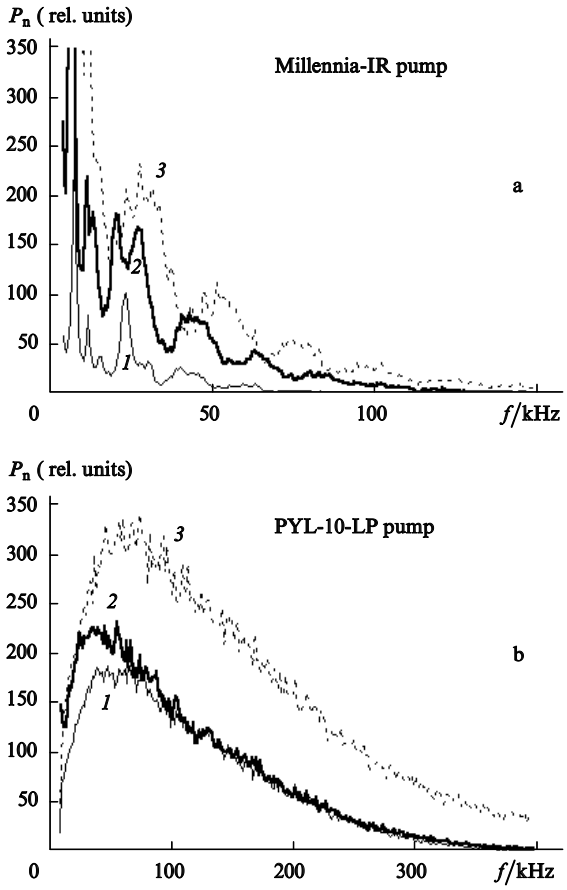

Figure 6. Spectra of the amplitude noises of the Cr^{4+} : forsterite laser and pump lasers Millennia-IR (a) and PYL-10-LP (b): noise of the pump laser (*1*) and the mode-locked Cr^{4+} : forsterite laser (*2*) and the Cr^{4+} : forsterite laser operating in the cw regime (*3*).

becomes an order of magnitude lower than upon pumping by the fibre laser (Fig. 6).

Our study also showed that the pump noise is converted to the lasing noise with some conversion coefficient. Note that the noise amplitude of both femtosecond lasers increased on passing to cw lasing. This means that, when femtosecond lasers are used in heterodyne measuring systems, a decrease in the sensitivity of detection of weak signals should be expected compared to that for standard heterodyne measurements with the use of cw sources operating with the shifted frequency of reference radiation, when the operating frequency range lies far beyond of the range of amplitude noises of the laser.

A decrease in the measurement sensitivity caused by the laser noise can be estimated taking into account that the ultimate sensitivity is determined by the shot noise of a photodetector

$$\overline{i_{\mathrm{sh}}^2} = 2eIF,$$

where e is the electron charge; $I = \eta eP/hv$ is the photodetector photocurrent; F is the noise bandwidth; P is the power of reference radiation of a heterodyne incident on the photodetector; hv is the energy of detected photons; and η is the quantum efficiency of the detector. Then, the ratio of the noise $\overline{i_{\mathrm{L}}^2}$ caused by the amplitude noise of the laser to the shot noise $\overline{i_{\mathrm{sh}}^2}$ will be determined by the expression

$$\frac{\overline{i_{\mathrm{L}}^2}}{\overline{i_{\mathrm{sh}}^2}} = \frac{\eta P_0 M^2}{2hvF_{\mathrm{L}}},$$

where M is the average value of the modulation degree in the frequency band F_{L}; and P_0 is the reference radiation power at which the shot noise exceeds the thermal noise of electronic devices.

Let us make the estimate for $M = 0.001$, $P_0 \approx 300$ μW, $v = 2.4 \times 10^{14}$ Hz, $F_{\mathrm{L}} \sim 100$ kHz, and $\eta = 0.3$. Then, we obtain that the noise caused by the amplitude fluctuations of laser radiation exceeds by a factor of 3×10^3 the shot noise, i.e., the sensitivity (the signal-to-noise ratio) will decrease by three orders of magnitude when such a laser is used. This estimate is made assuming that the spectral noise density is distributed uniformly within the 100-kHz band. If the Cr^{4+} : forsterite laser pumped by the PYL-10-LP laser is used, then, as follows from Fig. 6, the signal-to-noise ratio can be substantially increased by a proper choice of the frequency range. Thus, in the low-frequency region (up to 10 kHz), the sensitivity will increase by a factor of ten compared to the above estimate. For the heterodyne frequencies exceeding the noise bandwidth of the laser, the sensitivity of the system approaches the sensitivity corresponding to the shot noise limited regime.

At the same time, the use of a Cr^{4+} : forsterite laser pumped by a fibre laser for precision heterodyne measurements seems promising for the following reasons. First, the spectral characteristics of the amplitude noise of the laser pumped by a fibre laser make it more convenient for solving problems of optical coherent tomography, which are studied in the low-frequency region. Second, a pulse duration of 50 fs corresponds to a spatial resolution of ~ 15 μm, which is important for local Doppler measurements of flow velocities in biological scattering systems, for studying local fluctuations of the density and refractive index of liquids, etc. Finally, the frequency shift of a signal to the heterodyne region outside the noise bandwidth with the help of an acoustooptic modulator allows one to avoid the noise problem and to measure the velocity sign.

4. Conclusions

By using the domestic elemental base, we have developed and fabricated the femtosecond Cr^{4+} : forsterite laser pumped by a PYL-10-LP fibre laser equipped with an automated system for control of laser radiation parameters. We studied the spectrum of the amplitude noise of the femtosecond laser and discussed the possibilities of its use in heterodyne precision measurements of the dynamic characteristics of scattering objects.

Note that the use of efficient nonlinear optical frequency doublers in femtosecond Cr^{4+} : forsterite lasers [15] will permit measurements in the visible spectral range as well. Especially attractive for applications of femtosecond technologies, for example, in the eye microsurgery can be a combination of a cavity dumper [16], which provides an increase in the energy of an individual femtosecond pulse more than by an order of magnitude, retaining the average output power, with optical heterodyning used for a precision monitoring of the region subjected to operation.

Acknowledgements. This work was partially supported by the Russian Foundation for Basic Research (Grant Nos 00-02-17269 and 02-02-17238a).

References

1. Brezinski M., Fujimoto J. *IEEE J. Selected Topics Quantum Electron.*, **5**), 1185 (1999).
2. Gordienko V.M., Konovalov A.N., Magnitskii S.A., Tursynov Zh.S. *Kvantovaya Elektron.*, **31**, 83 (2001) [*Quantum Electron.*, **31**, 83 (2001)].
3. Bagayev S.N., Dmitriyev A.K., Chepurov S.V., et al. *Laser Phys.*, **11**, 1270 (2001).
4. Hell S., Bahlmann K., Shcreder M., et al. *J. Biomed. Opt.*, **1**, 61, 71 (1996).
5. *Proc. I–VIII Intern. Workshops Femtosecond Technology FST* (1994 – 2001, Tsukuba, Japan).
6. Bagayev S.N. *Kvantovaya Elektron.*, **31**, 377 (2001) [*Quantum Electron.*, **31**, 377 (2001)].
7. Seas A., Petricevic V., Alfano R. *Opt. Lett.*, **17**, 937 (1992).
8. Zhang Zh., Torizuka K., Itatani T., et al . *IEEE J. Quantum Electron.*, **33**, 1975 (1997).
9. Liu X., Qian L., Wise F. *Opt. lett.*, **23**, 129 (1998).
10. Ivanov A.A., Alfimov M.V., Zheltikov A.M. *Laser Phys.*, **10**, 796 (2000).
11. Gordienko V.M. *Preprint Mosk. Univ. (13)* (Moscow: 2000).
12. Gordienko V.M., Grechin S.S., Podshivalov A.A., Pryalkin V.I., Ivanov A.A. *Digest ICONO'2001* (SS3).
13. http//www.ire-polusgroup.com/
14. Tulin I.V. RF Patent No. 2057304, 18 May 1994.
15. Gordienko V.M., Ivanov A.A., Podshivalov A.A., Pryalkin V.I. *Kvantovaya Elektron.*, **31**, 341 (2001) [*Quantum Electron.*, **31**, 341 (2001)].
16. Slobodchikov E., Ma J., Kamalov V., Tominaga K., Yoshihara K. *Opt. Lett.*, **21**, 354 (1996).